Exploring Two-State Reactivity Pathways in the Cycloaddition Reactions of Triplet Methylene

Patricia Pérez,*,†,‡ J. Andrés,‡ V. S. Safont,‡ Renato Contreras,‡,§ and O. Tapia||

Departamento de Ciencias Químicas, Facultad de Ecología y Recursos Naturales, Universidad Andrés Bello, República 275, Santiago, Chile, Departament de Ciènces Experimentals, Universitat Jaume I, Box 224, 12080 Castelló, Spain, Departamento de Química, Facultad de Ciencias, Universidad de Chile, Casilla 653-Santiago, Chile, and Department of Physical Chemistry, Uppsala University, Box 579 75123 Upssala, Sweden

Received: November 19, 2004; In Final Form: March 20, 2005

Spin forbidden 1,2-cycloadditions of triplet methylene to alkenes have been theoretically studied as an example of the two-state reactivity paradigm in organic chemistry. The cycloadditions of triplet methylene to ethylene and the (*E*)- and (*Z*)-2-butene isomers show spin inversion after the transition state and therefore with no effect on the reaction rate. A local analysis shows that while triplet methylene addition to alkenes leading to the formation of a biradical intermediate is driven by spin polarization, the ring closure step to yield cyclopropane is a pericyclic process. We have found that at the regions in the potential energy surface where the spin crossover is likely to occur, the spin potential in the direction of increasing spin multiplicity, μ_S^+, tends to equalize the one in the direction of decreasing spin multiplicity, μ_S^-. This equalization facilitates the *spin transfer* process driven by changes in the spin density of the system.

Introduction

The discussion of reaction mechanisms is usually based on the analysis of a single potential energy surface with total spin conservation. For instance, a concerted process evolves from the minimum of the potential energy of reactants to the minimum potential energy associated to products through a single transition state. Eventually, the reaction may proceed through a more complex pathway, incorporating multiple transition-state structures and intermediates. Although this concept represents only one aspect of chemical reactivity, it has been very useful to rationalize a great number of chemical reactions. However, there are a wide variety of reactions in organic,[1,2] inorganic,[3,4] and organometallic chemistry[5−7] that involve a spin change in the transformation from reactants to products. In these cases, more than one state of different spin multiplicity must be incorporated in order to determine the minimum energy reaction pathway. Recently, the two-state reactivity (TSR) model was proposed to rationalize this kind of reactions.[8] According to this model, a thermal reaction involving spin crossover along the reaction coordinate connecting reactants to products must be described in terms of (at least) two-state reactivity. This is true if product formation arises from spin inversion interplay with the respective barrier heights on both spin surfaces. In this case, the system surfaces are strictly diabatic. The TSR model provides low energy paths, which may act as determinants in the kinetics and selectivity of the reaction.[8−12] Following Schröder et al.,[8] for the occurrence of TSR for a given set of reactants and products, some requirements must be fulfilled. The first one is a high spin state of the reactants and a low spin excited state which are separated by a low energy gap. Other prerequisites for the occurrence of TSR impose that the rate-determining transition-state structure arises from a spin multiplicity different than the reactant ground state.[13,14] An essential parameter to take into account is the intersection between the surfaces via spin−orbit coupling.[3] This parameter determines the probability of spin crossover.

Several authors have contributed to rationalize numerous processes involving multiple-state reactivity (MSR) in metallic complexes.[9−12] They showed that a spin change can introduce important thermodynamic and kinetic effects, not only in reactions of Werner-type compounds but also in middle valence and low valence organometallic compounds.[9] A computational study on ethylene C−H bond activation by the [(C_5Me_5)*Ir(PMe_3)] complex was recently reported.[12] The authors pointed out that the singlet surface intersects the triplet surface at multiple points, all lying at relatively low energies, so that crossover to the singlet state should be relatively facile. The results are in agreement with the product distribution 2:1 in favor of the formation of vinyl hydride with respect to the formation of an ethylene complex.[12]

From a theoretical point of view, the location of the crossing points (CPs) between potential energy surfaces of different spin multiplicities is of fundamental importance. Harvey et al.[15] have developed an algorithm to find the minimum energy CP. Even though the existence of a CP structure has been used to explain the kinetics and the product distribution in a significant number of cases, it cannot be associated to a well-defined chemical species; this point is not stationary. The TSR paradigm has its foundation in the spin−orbit coupling; spin is usually related to a relativistic effect, and in this sense, it may be important even for reactivity involving light atoms. At the CP region of the diabatic potential energy surfaces (PESs), what we probably have is a state for which the wave function is a linear superposition that is no longer an eigenfunction of the total spin operator. Here, we still may define a state for which the total angular moment $\mathbf{J} = \mathbf{L} + \mathbf{S}$ is conserved and $\mathbf{J}^2 = \mathbf{L}^2 + \mathbf{S}^2 + 2\mathbf{L}\cdot\mathbf{S}$. In other words, at the CP region, there might be a number

† Universidad Andrés Bello.
‡ Universitat Jaume I.
§ Universidad de Chile.
|| Uppsala University.

10.1021/jp044701k CCC: $30.25 © 2005 American Chemical Society
Published on Web 04/16/2005

of states, represented by the diabatic PESs (two for the TSR), that are accessible to the system; they are coupled by the **L**•**S** term and mixed. Consequently, the resulting superposition does not conserve the spin multiplicity of the starting state. In the resonance case, these states are equally accessible.[16] Spin−orbit coupling opens channels of different spin only around such a region. The effect is taken for granted, and the important factor will be to identify such cross points accurately. In this work, we present a different approach to the TSR paradigm, which is based on an empirical principle of spin potential equalization (SPE). SPE is similar to the electronegativity equalization principle introduced in the description of the one-state reactivity case. The model will be illustrated for the spin forbidden 1,2-cycloaddition of triplet methylene to ethylene and the *E* and *Z* isomers of 2-butene to afford cyclopropanes in the singlet state.[16] Additionally, the stereochemistry of these processes has been rationalized by the Skell hypothesis,[17] stating that since singlet carbenes add to alkenes in a single concerted process, the addition is always stereospecific. Cycloaddition of triplet carbenes on the other hand cannot give cyclopropane in a one-step process because this reaction is spin forbidden, and it must occur in a two-step process, via a biradical intermediate. This intermediate must undergo spin inversion before the second C−C bond is formed.[18] Whether or not the alkene stereochemistry is preserved depends on the relative speed of the spin inversion versus C−C bond rotation processes.[18] Spin inversion involves the participation of more than a single spin surface connecting reactants and products, and spin crossover along the reaction coordinate may occur, if the propensity of the system to change its spin multiplicity is facilitated by the SPE principle introduced here.

Previous theoretical works concerning reaction paths for the addition of simple carbenes to alkenes have been presented. For instance, Engels et al.[19] have used the minimum energy paths (MEP) model to study the reaction of singlet and triplet methylene with ethylene. These authors found that the change from the triplet to singlet surface may occur at large separations of the CH_2 and C_2H_4 fragments. Hoffmann et al.[20] have presented a detailed study on the methylene−ethylene surface, stressing the importance of the choice of the computational reaction coordinate. On the other hand, Kutzelnigg and Zurawski[21] studied the reaction path for the addition of singlet methylene to ethylene to yield cyclopropane. These authors found that the energy along the reaction path decreases monotonically without barrier. Shevlin et al.[22] have presented a computational study of the reactions of methylene and chloro- and dichloro-carbene with cyclopropane. In all three cases, the lowest energy reaction path between the carbene and cyclopropane was predicted to be a C−H insertion. It is important to stress that, in these previous works, the origin of the spin crossover has not been addressed in detail.

Model Equations

It is well-known that the spin-polarized version of density functional theory (DFT-SP) can improve the description of the electronic structure of atoms, molecules, and solids[23] by breaking the electronic density into spin components, namely, $\rho(\mathbf{r}) = \rho_\uparrow(\mathbf{r}) + \rho_\downarrow(\mathbf{r})$. In this notation, $\uparrow$ refers to spin-up (α) spaces and $\downarrow$ refers to spin-down (β) spaces. The formulation of the spin-polarized DFT theory developed by Galván, Vela, Vargas, and Gázquez[24−26] has introduced a complete set of independent functions that can be expressed in terms of the electronic density, $\rho(\mathbf{r})$, and the spin density, $\rho_S(\mathbf{r})$. The latter quantity is defined by $\rho_S(\mathbf{r}) = \rho_\uparrow(\mathbf{r}) - \rho_\downarrow(\mathbf{r})$. The α and β spin densities obey the following normalization conditions:

$$\int \rho_\uparrow(\mathbf{r})\, d\mathbf{r} = N_\uparrow \tag{1a}$$

$$\int \rho_\downarrow(\mathbf{r})\, d\mathbf{r} = N_\downarrow \tag{1b}$$

$$\int \rho(\mathbf{r})\, d\mathbf{r} = N_\uparrow + N_\downarrow = N \tag{2}$$

and

$$\int \rho_S(\mathbf{r})\, d\mathbf{r} = N_\uparrow - N_\downarrow = N_S \tag{3}$$

where N_S defines the spin number (i.e., the number of unpaired spins). Within this formalism, the total energy, E, for the system is expressed as a functional of the electronic density, $\rho(\mathbf{r})$, the spin density, $\rho_S(\mathbf{r})$, the external potential, $v(\mathbf{r})$, and an external magnetic field, $\mathbf{B}(\mathbf{r})$, namely,[24−26]

$$E[\rho,\rho_S,v(\mathbf{r}),\mathbf{B}(\mathbf{r})] = F[\rho,\rho_S] + \int \rho(\mathbf{r})\, v(\mathbf{r})\, d\mathbf{r} - \mu_B \int \rho_S(\mathbf{r})\, \mathbf{B}(\mathbf{r})\, d\mathbf{r} \tag{4}$$

where μ_B is the Bohr magneton. The generalized Hohenberg−Kohn functional, $F[\rho,\rho_S]$, includes the electronic kinetic energy and electronic repulsion, incorporating exchange-correlation effects.[27] Minimization of the energy functional of eq 4 with respect to $\rho(\mathbf{r})$ and $\rho_S(\mathbf{r})$ under normalization conditions 2 and 3 and omitting $\mathbf{B}(\mathbf{r})$ as a first approximation leads to the following Euler equations:[24−26]

$$\mu_N = \left(\frac{\delta E}{\delta \rho(\mathbf{r})}\right)_{\rho_S,v} \tag{5}$$

and

$$\mu_S = \left(\frac{\delta E}{\delta \rho_S(\mathbf{r})}\right)_{\rho,v} \tag{6}$$

μ_N is similar (but not equal) to the electronic chemical potential defined in the spin-restricted case. μ_S is defined as the spin potential of the system, and it may be related to the propensity of a system to change its spin polarization. The quantity defined in eq 6 separates into two terms, the spin potentials μ_S^- and μ_S^+ in the direction of decreasing and increasing multiplicity, respectively. They may be approximately expressed as

$$\mu_S^- = \frac{(\epsilon_H^\alpha(M') - \epsilon_L^\beta(M'))}{2} \tag{7}$$

and

$$\mu_S^+ = \frac{(\epsilon_L^\alpha(M) - \epsilon_H^\beta(M))}{2} \tag{8}$$

These terms can be evaluated using the finite difference formulas proposed by Galván et al.,[25,26] in terms of the frontier molecular orbitals HOMO and LUMO, for the system in the lower and upper M and M' spin multiplicities in the α and β axes.[28] The 2-spinor electron state has as base vectors $\alpha \rightarrow (1\ 0)$ and $\beta \rightarrow (0\ 1)$.

Two additional global quantities that are useful for discussing energy changes associated to change in spin multiplicity are the spin-philicity and spin-donicity numbers.[28] They are defined as $\omega_S^+ = (\mu_S^+)^2/2\eta_{SS}$ and $\omega_S^- = (\mu_S^-)^2/2\eta_{SS}$, respectively.[28]

$\eta_{SS} = (\mu_S^- - \mu_S^+)/2$ is the spin hardness, a quantity describing the resistance of the system to change its spin multiplicity.[26]

A set of generalized local reactivity indexes may provide additional information, in the form of reactivity indices defined for atoms or (functional) groups. They are useful for assessing the responses of the electronic and spin densities of a molecular system with respect to the variations in the number of electrons and multiplicity. They are[24−26]

$$f_{NN}(\mathbf{r}) = \left(\frac{\partial \rho(\mathbf{r})}{\partial N}\right)_{N_S, v(\mathbf{r})} \tag{9}$$

$$f_{SN}(\mathbf{r}) = \left(\frac{\partial \rho_S(\mathbf{r})}{\partial N}\right)_{N_S, v(\mathbf{r})} \tag{10}$$

$$f_{NS}(\mathbf{r}) = \left(\frac{\partial \rho(\mathbf{r})}{\partial N_S}\right)_{N, v(\mathbf{r})} \tag{11}$$

and

$$f_{SS}(\mathbf{r}) = \left(\frac{\partial \rho_S(\mathbf{r})}{\partial N_S}\right)_{N, v(\mathbf{r})} \tag{12}$$

Within this approximation, while $f_{NN}(\mathbf{r})$ will provide information about the initial response of the system to charge transfer, $f_{SS}(\mathbf{r})$ will provide information about the change in the spin densities with respect to changes in the spin numbers. The latter Fukui function is named the spin Fukui function.

In the present approach, we are interested in the generalized Fukui functions in the direction of increasing and decreasing N (f_{NN}^+ and f_{NN}^-) as well as in the direction of increasing and decreasing spin multiplicity (f_{SS}^+ and f_{SS}^-). They may be approached as follows:[25]

$$f_{NN}^+(\mathbf{r}) \cong {}^1/_2[|\Phi_{LUMO}^{\alpha}(\mathbf{r})|^2 + |\Phi_{LUMO}^{\beta}(\mathbf{r})|^2] \tag{13a}$$

$$f_{NN}^-(\mathbf{r}) \cong {}^1/_2[|\Phi_{HOMO}^{\alpha}(\mathbf{r})|^2 + |\Phi_{HOMO}^{\beta}(\mathbf{r})|^2] \tag{13b}$$

$$f_{SS}^+(\mathbf{r}) \cong {}^1/_2[|\Phi_{LUMO}^{\alpha}(\mathbf{r})|^2 + |\Phi_{HOMO}^{\beta}(\mathbf{r})|^2] \tag{14a}$$

$$f_{SS}^-(\mathbf{r}) \cong {}^1/_2[|\Phi_{HOMO}^{\alpha}(\mathbf{r})|^2 + |\Phi_{LUMO}^{\beta}(\mathbf{r})|^2] \tag{14b}$$

Computational Details

The PESs of the three reactions considered were calculated at the (U)B3LYP/6-31G(d) level of theory using the Gaussian 98 suite of programs.[29] The intrinsic reaction coordinate (IRC)[30] method has been used to describe the minimum energy paths connecting the TSs with the corresponding minima. Structures of the three different singlet−triplet crossing points were found using Harvey's algorithm.[15] In this methodology, the search of the minimum energy crossing points (MECPs) between noninteracting PESs requires energies and analytical energy gradients between both hypersurfaces involved. Starting from the TS closest to the crossing seams, the reaction pathway may be traced down to the corresponding minimum. Thereafter, each point optimized along the IRC path is submitted to a single point energy calculation with the other spin multiplicity. In this manner, it is possible to obtain structures of the CPs that have identical geometry and energy in the singlet and triplet states.[15] This algorithm has been previously used in the study of gas-phase reactions of organometallic systems.[6b,31]

The calculation of the Fukui functions was performed by a method described elsewhere,[32,33] that evaluates this quantity condensed to atoms or groups, in terms of the coefficients of the frontier molecular orbitals involved and the overlap matrix.

TABLE 1: Relative Energies, ΔE, in kcal/mol for the Three Reactions under Study

species	ΔE^a	ΔE^b
Reaction: Ethylene + Triplet Methylene → Cyclopropane		
R-0 (S)	13.4	17.1
R-0 (T)	0.0	0.0
TS-0 (T)	1.6	7.6
CP-0	−34.0	−35.8
I-0 (T)	−37.6	−36.1
P-0 (S)	−98.6	−103.6
Reaction: (*Z*)-2-Butene + Triplet Methylene → *cis*-1,2-Dimethylcyclopropane		
R-1 (S)	13.7	21.0
R-1 (T)	0.0	0.0
TS-1 (T)	3.8	12.3
CP-1	−30.5	−33.6
I-1 (T)	−34.3	−33.7
P-1 (S)	−93.9	−97.5
Reaction: (*E*)-2-Butene + Triplet Methylene → *trans*-1,2-Dimethylcyclopropane		
R-2 (S)	13.6	20.9
R-2 (T)	0.0	0.0
TS-2 (T)	2.5	12.4
CP-2	−31.7	−27.5
I-2 (T)	−34.7	−30.3
P-2 (S)	−95.3	−98.8

[a] Relative energies evaluated at the B3LYP/6-31G(d) level of theory. [b] Relative energies evaluated at the MP2/6-31G(d)//B3LYP/6-31G(d) level of theory.

Results and Discussion

The structures of the relevant stationary points and the respective CPs of the three reactions studied are depicted in Figure 1. To identify the different structures involved in the present study, the following nomenclature will be used hereafter. The general structure is **Z-X** (**S** or **T**, for singlet or triplet multiplicity), where **Z** represents any of the stationary points corresponding to reactants (**R**), products (**P**), intermediates (**I**), transition states (**TS**), and the (not stationary) crossing points (**CP**). **X = 0** corresponds to the ethylene and triplet methylene reaction; **X = 1** corresponds to the (*Z*)-2-butene and triplet methylene reaction, and **X = 2** corresponds to the (*E*)-2-butene and triplet methylene reaction. For the 1,2-cycloaddition of methylene to ethylene (see Table 1), the low-lying pathway corresponding to the triplet channel is characterized by a transition-state structure (**TS-0 (T)**) connecting reactants (**R-0 (T)**) and a biradical intermediate (**I-0 (T)**), with a calculated barrier of 1.6 kcal/mol which is lower than the experimental value 5.3 kcal/mol.[34] This result is not surprising, as the UB3LYP method is known to predict energy barriers lower than the experimental ones. However, a correction of the reaction barrier at the UMP2/6-31G(d)//UB3LYP/6-31G(d) level yields a value of 7.6 kcal/mol, that is, closer to the experiment (see Table 1, third column). The singlet channel shows a barrierless pathway directly connecting reactants (**R-0 (S)**, 17.1 kcal/mol higher than the triplet reactants at the MP2 level) and products (**P-0 (S)**, cyclopropane). Using the information taken from the intrinsic reaction coordinate (IRC) analysis for the triplet pathway and a surface scan for the singlet channel as input, we performed a crossing point search using the algorithm proposed by Harvey et al.[15] The schematic profile including the **CPs** is sketched in Figure 2, for the three cycloaddition reactions studied here. It may be seen that **CP-0** is located after the triplet

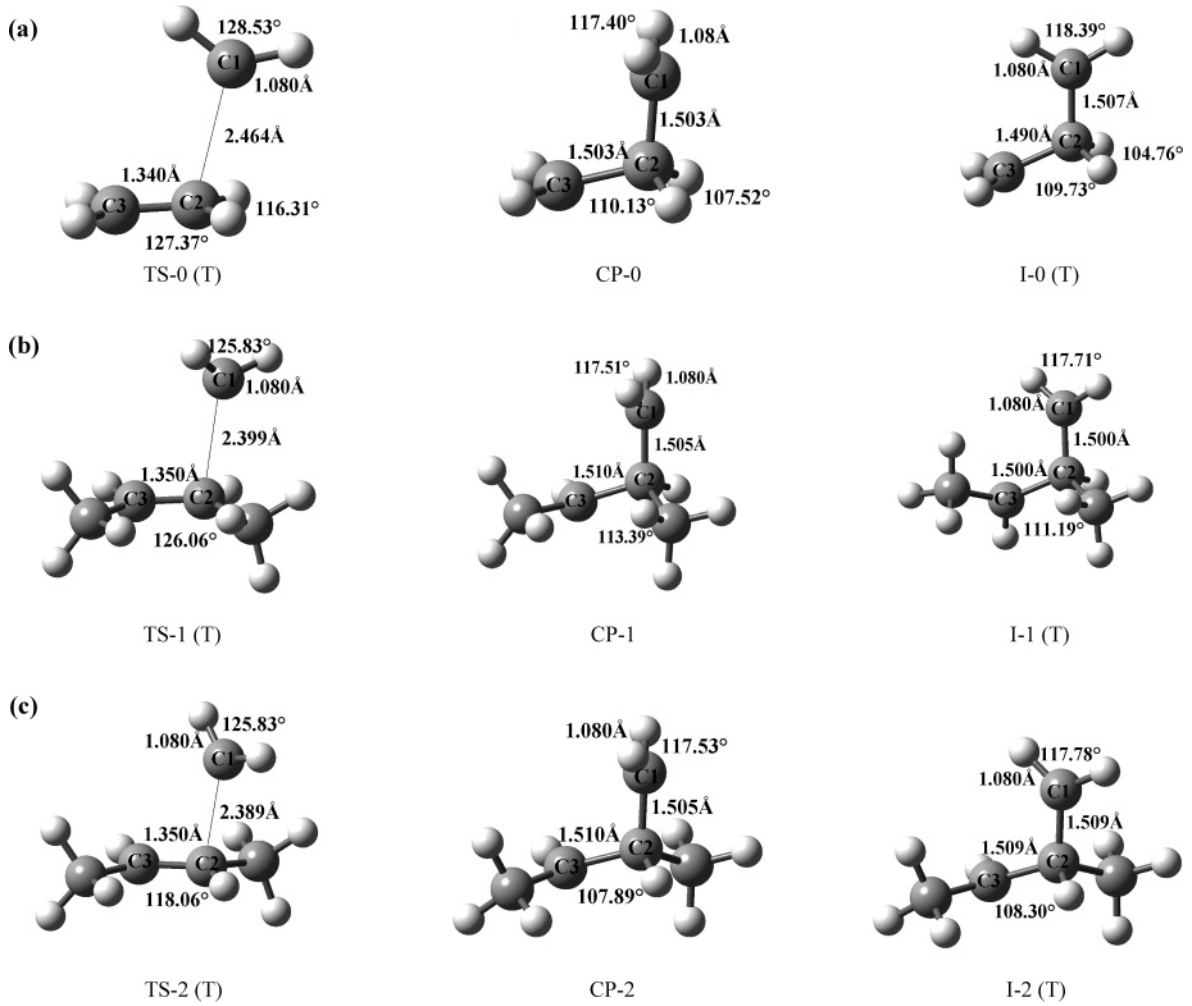

Figure 1. Geometrical parameters for the addition of triplet methylene to (a) ethylene, (b) (*Z*)-butene, and (c) (*E*)-butene and atom numbering.

transition-state structure, and therefore with no net effect on the reaction rate.

The analysis of the 1,2-cycloadditions of triplet methylene to the (*Z*)- and (*E*)-2-butene isomers shows similar patterns. The PES for the cycloaddition of triplet methylene to (*Z*)-2-butene is characterized by a transition-state (**TS-1 (T)**) structure with a predicted reaction barrier to the biradical intermediate (**I-1 (T)**) of 3.8 kcal/mol at the UB3LYP/6-31G(d) level (corrected to 12.3 kcal/mol at the UMP2/6-31G(d)//UB3LYP/6-31G(d) level, see Table 1). The singlet and triplet channels including **CP-1** and the **I-1 (T)** are also sketched in Figure 2. The singlet channel shows again a barrierless pathway directly connecting reactants (**R-1 (S)**, 13.7 kcal/mol higher than the triplet reactants at the B3LYP/6-31G(d) level of theory) and products (**P-1 (S)**, *cis*-1,2-dimethylcyclopropane). **CP-1** was located after the formation of the **TS-1 (T)** structure, at a reaction stage prior to the formation of the triplet biradical intermediate (**I-1 (T)**), and therefore with no effect on the reaction rate but with a significant effect on the stereochemistry of the cycloaddition. In fact, a full geometry relaxation from **CP-1** along the singlet spin multiplicity leads to the *cis*-1,2-dimethylcyclopropane ground state, where the stereochemistry of the alkene has been preserved.

Full geometry relaxation from **CP-1** in the triplet spin multiplicity on the other hand leads to the triplet biradical intermediate species. However, in this case, it is not possible to asses the stereochemistry of products along the triplet channel. As stated by the Skell hypothesis, the cycloaddition of triplet carbenes is not stereospecific. If rotation around the C−C bond is faster than spin crossover, then the stereochemistry of the starting material is not retained. Spin crossover depends on spin−orbit coupling, which is expected to be small in the present case, so that the crossover should be slow, at least slower than bond rotation.[35] We have further explored the potential energy surface for the addition of triplet methylene to (*E*)- and (*Z*)-2-butene in order to obtain an estimate of the barrier for rotation around the C−C bond. The attempts to locate a transition-state structure failed. A scan made for the torsional angle involved in this rotation gives a barrier of about 1.2 kcal/mol calculated with reference to the maximum energy rotamer found in the scan. The scan energy profile and the structure of this rotamer are shown in Figure 3. This result suggests that the rotation around the C−C bond may be faster than spin-state change and ring closure.

The schematic reaction profile for the 1,2-cycloaddition of methylene to (*E*)-2-butene is also sketched in Figure 2 (see Table 1 for relative energies at the UB3LYP/6-31G(d) and UMP2/6-31G(d)//UB3LYP/6-31G(d) levels). It may be seen that spin crossover at **CP-2** occurs after the formation of the **TS-2 (T)** structure and before the formation of the triplet biradical intermediate (**I-2 (T)**), and therefore with no effect on the reaction rate (see Table 1). Full geometry relaxation from **CP-2** along the singlet spin multiplicity leads to the *trans*-1,2-dimethylcyclopropane **P-2 (S)** ground state, where the stereochemistry of the alkene has been again preserved. Full geometry relaxation from **CP-2** in the triplet spin multiplicity on the other

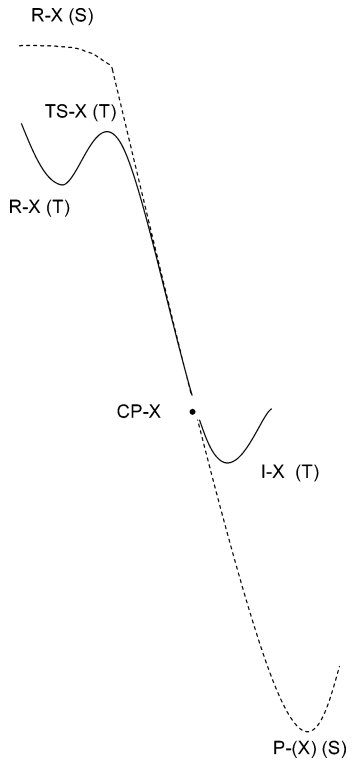

Figure 2. Schematic profiles for the addition of triplet methylene to singlet ethylene, (*Z*)-butene, and (*E*)-butene. Relative energies are quoted in Table 1 for each stationary point for the reactions under study.

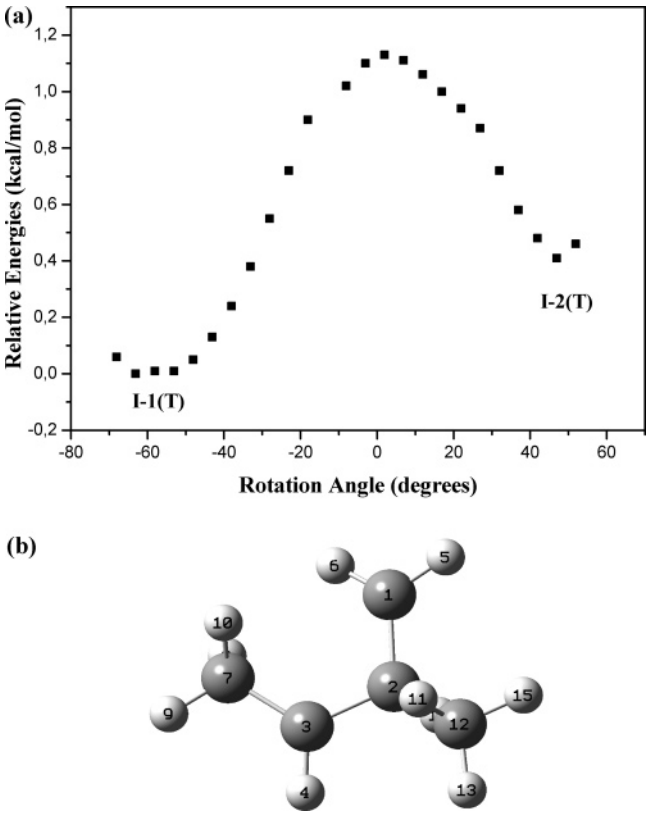

Figure 3. (a) Energy profile from the scan on the torsional angle C7C3C2C1 and (b) structure of the maximum energy rotamer from part a for which the torsional angle is C7C3C2C1 = 1.94 °.

hand leads to the **I-2 (T)** species. In summary, the TSR analysis based on energetic aspects predicts that the singlet−triplet crossing has no effect on the reaction rates for the 1,2-cycloadditions of triplet methylene to the *E* and *Z* isomers of 2-butene. It also confirms the Skell hypothesis in the case of the stereochemistry expected for the cycloaddition of the singlet carbene. However, the stereochemistry for the addition of triplet carbene cannot be assessed, as the relaxation from **CP-1** and **CP-2** leads to the corresponding intermediates **I-1 (T)** and **I-2 (T)**, respectively.

TABLE 2: Global Spin Quantities for the Analysis of the 1,2-Cycloaddition Reaction of Triplet Methylene to Alkenes (Singlet−Triplet Energy Gap, ΔE (S−T), in kcal/mol and Other Quantities in eV at the B3LYP/6-31G(d) Level of Theory)

species	ΔE (S−T)	μ_S^+	μ_S^-	$\Delta\mu_S^{\pm}$ [a]	ω_S^- [b]
Reaction: Ethylene + Triplet Methylene → Cyclopropane					
R-0 (T)	13.4		−2.254	−0.598	1.299
R-0 (S)		1.656			
TS-0 (T)	35.3		−2.094	−1.519	1.643
TS-0 (S_v)		0.575			
CP-0 (T)	0.0		−1.427	0.0130	0.710
CP-0 (S)		1.440			
Reaction: (*Z*)-2-Butene + Triplet Methylene → *cis*-1,2-Dimethylcyclopropane					
R-1 (T)	13.7		−2.257	−0.744	1.351
R-1 (S)		1.513			
TS-1 (T)	40.5		−1.946	−1.588	1.644
TS-1 (S_v)		0.358			
CP-1 (T)	0.0		−1.347	0.030	0.666
CP-1 (S)		1.377			
Reaction: (*E*)-2-Butene + Triplet Methylene → *trans*-1,2-Dimethylcyclopropane					
R-2 (T)	13.6		−2.257	−0.744	1.352
R-2 (S)		1.513			
TS-2 (T)	39.4		−1.946	−1.529	1.603
TS-2 (S_v)		0.417			
CP-2 (T)	0.0		−1.346	0.027	0.666
CP-2 (S)		1.373			

[a] $\Delta\mu_S^{\pm} = \mu_S^+ + \mu_S^-$. TS-X ($S_v$; **X** = 0,1,2) is the vertical transition-state structure. [b] ω_S^- corresponds to the spin-donicity number of the triplet states. See the text for details.

On the other hand, Table 2 shows the values of the spin potential (μ_S^+ and μ_S^-) in the most important points of the reaction coordinate. It may be seen that the lowest singlet−triplet spin potential difference, $\Delta\mu_S^{\pm}$, is attained at the crossing point of the surface (Table 2, fifth column). This result suggests that a spin potential equalization rule may account for the spin crossover. We claim that at the regions in the PES where the spin crossover is likely to occur, namely, the CP region, the spin potential in the direction of increasing spin multiplicity, μ_S^+, must equalize the one in the direction of decreasing spin multiplicity, μ_S^-. This equalization facilitates the *spin transfer* process driven by ΔN_S. Therefore, instead of calculating potential energy crossing points, we sense them with these new quantities. Note that the spin-donicity index, ω_S^-,[28] shows its highest values at the triplet transition-state structures. Remember that, at this stage of the reaction, the minimum energy pathway goes along the triplet channel in all three systems studied. In other words, while the activation for spin transfer measured by the spin-philicity/spin-donicity parameters is being prepared earlier at the TS, the spin polarization process is more likely to occur at the crossing point, where the spin potentials in both increasing and decreasing multiplicity directions tend to equalize (see Table 2).

To analyze the polar or nonpolar character of the cycloaddition reactions under study and the local spin polarization effects, the calculation of the electronic and spin-polarized Fukui functions described in eqs 13 and 14 was performed at the

TABLE 3: Electronic and Spin Fukui Functions in the Direction of Increasing N and N_S (+) and in the Direction of Decreasing N and N_S (−)[a]

species	site (k)	f^+_{NN}	f^-_{NN}	f^+_{SS}	f^-_{SS}
Reaction: Ethylene + Triplet Methylene → Cyclopropane					
TS-0 (T)	C1	0.344	0.286	0.065	0.565
	C2	0.303	0.313	0.565	0.050
	C3	0.322	0.371	0.359	0.334
CP-0 (T)	C1	0.243	0.292	0.052	0.480
	C2	0.000	0.126	0.109	0.015
	C3	0.243	0.292	0.052	0.480
CP-0 (S)	C1	0.490	0.470		
	C2	0.018	0.012		
	C3	0.490	0.470		
Reaction: (*Z*)-2-Butene + Triplet Methylene → *cis*-1,2-Dimethylcyclopropane					
TS-1 (T)	C1	0.333	0.261	0.083	0.512
	C2	0.260	0.272	0.479	0.053
	C3	0.289	0.331	0.283	0.338
CP-1 (T)	C1	0.272	0.191	0.028	0.435
	C2	0.000	0.103	0.092	0.013
	C3	0.186	0.336	0.054	0.468
CP-1 (S)	C1	0.459	0.488		
	C2	0.013	0.013		
	C3	0.471	0.392		
Reaction: (*E*)-2-Butene + Triplet Methylene → *trans*-1,2-Dimethylcyclopropane					
TS-2 (T)	C1	0.333	0.259	0.082	0.510
	C2	0.264	0.268	0.481	0.052
	C3	0.295	0.330	0.282	0.344
CP-2 (T)	C1	0.271	0.199	0.038	0.433
	C2	0.000	0.113	0.092	0.000
	C3	0.185	0.335	0.053	0.467
CP-2 (S)	C1	0.460	0.484		
	C2	0.012	0.012		
	C3	0.463	0.394		

[a] See Figure 1 for atom numbering.

transition states (**TS-X (T)**; **X** = 0,1,2). The results are summarized in Table 3. The electrophilic and nucleophilic Fukui functions at site k, f^+_{NN} and f^-_{NN}, respectively, describing the most electrophilic and nucleophilic reactive sites are shown in the third and fourth columns for the three cycloaddition processes studied here. The highest values of f^+_{NN} are located at the carbon site C1 of the methylene moiety and at the carbon C3 of the alkene end for f^-_{NN}. These sites are directly involved in the ring closure process leading to cyclopropanes. The polarity of cycloadditions may be conveniently described in terms of the difference in electrophilicity/nucleophilicity of the interacting pairs.[36] In the present case, the electronic Fukui functions f^+_{NN} and f^-_{NN} bear this information, and therefore, their difference may be used to estimate the degree of polarity in the C1−C3 interaction involved in the ring closure step. From the values quoted in Table 3, it may be verified that, in the cases studied here, this difference is small, and therefore, the ring closure process may be described as nonpolar.

In chemical processes where more than one energy surface is involved, the local reactivity picture must be complemented with additional reactivity indexes which are defined with respect to the variations of spin density. The spin Fukui functions f^+_{SS} and f^-_{SS} defining the changes in spin density in the direction of increasing and decreasing multiplicity, respectively, carries useful information about local or regional reactivity (intramolecular selectivity).[24−26] The calculated values of f^+_{SS} and f^-_{SS} are summarized in Table 3, columns 5 and 6. In the three reactions studied, it may be seen that the highest values are located at centers C1 and C2 of **TS-X (T)**, which are involved in the process of forming the triplet biradical. Note that the active sites in the process of formation of the triplet biradical are characterized by high values of f^+_{SS} at the alkene moiety (C2) and f^-_{SS} at the methylenic C1 site. This result indicates that the formation of the biradical triplet (**I−X (T)**) is mostly driven by changes in the spin density rather than the electrophilic and nucleophilic Fukui functions f^+_{NN} and f^-_{NN} at sites C1 and C3, respectively. Our results summarized in Scheme 1 show that while methylene addition to alkenes to afford the biradical intermediate is driven by spin polarization, the ring closure process to cyclopropane is a pericyclic (i.e., nonpolar) process. The usefulness of the generalized Fukui function analysis is granted by the fact that it incorporates the important changes in the spin density along the reaction channel. This fact has been recently recognized by Griesbeck et al. in the study of selectivity control in electron spin inversion processes.[37] These authors state that while in a classical organic reaction involving (closed shell) ground states of reactants and products the electron spin is a negligible quantity, in the chemistry of carbene cycloadditions, changes between spin states completely determine the rate and selectivity of the process. In the present approach, the generalized Fukui functions describe an intramolecular selectivity which may be driven by changes in the electron density, in the spin density, or in both.

SCHEME 1: Biradical Formation and Ring Closure Process in Terms of Spin Transfer and Polarity of the Cycloadditions

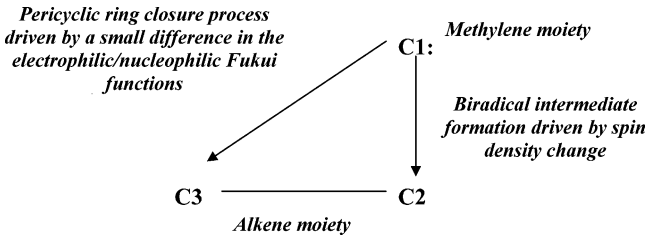

Concluding Remarks

The TSR analysis based on energetic aspects predicts that the singlet−triplet crossing has no effect on the reaction rates for the 1,2-cycloadditions of triplet methylene to the *E* and *Z* isomers of 2-butene. The Skell hypothesis regarding the stereochemistry expected for the cycloaddition of the singlet methylene is confirmed. However, the stereochemistry for the addition of triplet methylene cannot be assessed, because the relaxation from the corresponding crossing points leads to the biradical intermediates (**I-1 (T)** and **I-2 (T)**), respectively.

Additional results show that that at the regions in the potential energy surface where the spin crossover is likely to occur, the spin potential in the direction of increasing spin multiplicity, μ^+_S, tends to equalize the one in the direction of decreasing spin multiplicity, μ^-_S. This equalization that facilitates the *spin transfer* process driven by changes in the spin density of the system may play a key role in spin forbidden reactions. On the other hand, the use of generalized Fukui functions, incorporating changes in both the electron and spin densities, opens an interesting alternative to explore selectivity and stereochemistry in TSR problems.

Acknowledgment. This work was supported by Fondecyt grants 1020069 and 1030548, project DI-15-04 from UNAB, Millennium Nucleus for Applied Quantum Mechanics and Computational Chemistry, and project P02-004-F (MIDEPLAN and CONICYT). O.T. thanks Fondecyt, grant 7020069, for

financial support. J.A. and V.S.S. acknowledge the DGI, project BQU2003-04168-C03-03, and the GV, project GRUPOS02-028. The authors acknowledge Professor Marcelo Galván for encouraging discussions involving the equalization of spin potentials.

References and Notes

(1) Yoshizawa, K.; Shiota, Y.; Yamabe, T. *J. Am. Chem. Soc*. **1999**, *121*, 147.

(2) Wilsey, S.; Bernardi, F.; Olivucci, M.; Robb, M. A.; Murphy, S.; Adam, W. *J. Phys. Chem. A* **1999**, *103*, 1669.

(3) (a) Danovich, D.; Shaik, S. *J. Am. Chem. Soc*. **1997**, *119*, 1773. (b) Filatov, M.; Shaik, S. *J. Phys. Chem. A* **1998**, *102*, 3835.

(4) Rue, C.; Armentrout, P. B.; Schwarz, H. *J. Chem. Phys.* **1999**, *110*, 7858.

(5) Hess, J. S.; Leelasubcharoen, S.; Rheingold, A. L.; Doren, D. J.; Theopold, K. H. *J. Am. Chem. Soc*. **2002**, *124*, 2454.

(6) (a) Gracia, L.; Sambrano, J. R.; Safont, V. S.; Calatayud, M.; Beltrán, A.; Andrés, J. *J. Phys. Chem. A* **2003**, *107*, 3107. (b) Gracia, L.; Andrés, J.; Safont, V. S.; Beltrán, A.; Sambrano, J. R. *Organometallics* **2004**, *23*, 730.

(7) Poli, R.; Harvey, J. N. *Chem. Soc. Rev.* **2003**, *32*, 1.

(8) Schröder, D.; Shaik, S.; Schwarz, H. *Acc. Chem. Res*. **2000**, *33*, 139.

(9) Poli, R. *Chem. Rev.* **1996**, *96*, 2135.

(10) Harvey, J. N.; Poli, R.; Smith, K. M. *Coord. Chem. Rev*. **2003**, *238*/*239*, 347.

(11) Poli, P. *Acc. Chem. Res*. **1997**, *30*, 494.

(12) Smith, K. M.; Poli, R.; Harvey, J. N. *Chem.*—*Eur. J*. **2001**, *7*, 1679.

(13) Irigoras, A.; Fowler, J. E.; Ugalde, J. *J. Am. Chem. Soc*. **1999**, *121*, 8549.

(14) Schröder, D.; Schwarz, H. *Angew. Chem., Int. Ed. Engl*. **1995**, *34*, 1973.

(15) Harvey, J. N.; Aschi, M.; Schwarz, H.; Koch, W. *Theor. Chem. Acc*. **1998**, *99*, 95.

(16) Moody, C. J.; Whithman, G. H. *Reactive Intermediates*; Oxford University Press, Oxford Chemistry Primers: Oxford, New York, 1997.

(17) (a) Skell, P. S.; Garner, A. Y. *J. Am. Chem. Soc*. **1956**, *78*, 3409. (b) Skell, P. S.; Woodworth, R. C. *J. Am. Chem. Soc*. **1956**, *78*, 4496. (c) Skell, P. S.; Garner, A. Y. *J. Am. Chem. Soc.* **1956**, *78*, 5430.

(18) Moss, R. A., Platz, M. S., Jones, M., Jr., Eds. *Reactive Intermediate Chemistry*; John Wiley & Sons: 2004.

(19) Reuter, W.; Engels, B.; Peyerimhoff, S. D. *J. Phys. Chem*. **1992**, *96*, 6221.

(20) Hoffmann, R.; Hayes, D. M.; Skell, P. S. *J. Phys. Chem.* **1972**, *76*, 664.

(21) Zurawski, B.; Kutzelnigg, W. *J. Am. Chem. Soc.* **1978**, *100*, 2654.

(22) Sevin, F.; McKee, M. L.; Shevlin, P. B. *J. Org. Chem.* **2004**, *69*, 382.

(23) Slater J. C. *Quantum Theory of Molecules and Solids*; McGraw-Hill: New York, 1974; Vol. 4.

(24) Vargas, R.; Galván, M. *J. Phys. Chem.* **1996**, *100*, 14651.

(25) Galván, M.; Vela, A.; Gázquez, J. L. *J. Phys. Chem.* **1988**, *92*, 6470.

(26) Vargas, R.; Galván, M.; Vela, A. *J. Phys. Chem. A* **1998**, *102*, 3134.

(27) Hohenberg, P.; Kohn, W. *Phys. Rev. B* **1964**, *136*, 864.

(28) Pérez, P.; Andrés, J.; Safont, V. S.; Tapia O.; Contreras R. *J. Phys. Chem. A* **2002**, *106*, 5353.

(29) Frisch, M. J.; Trucks, G. W.; Schlegel, H. B.; Scuseria, G. E.; Robb, M. A.; Cheeseman, J. R.; Zakrzewski, V. G.; Montgomery, J. A., Jr.; Stratmann, R. E.; Burant, J. C.; Dapprich, S.; Millam, J. M.; Daniels, A. D.; Kudin, K. N.; Strain, M. C.; Farkas, O.; Tomasi, J.; Barone, V.; Cossi, M.; Cammi, R.; Mennucci, B.; Pomelli, C.; Adamo, C.; Clifford, S.; Ochterski, J.; Petersson, G. A.; Ayala, P. Y.; Cui, Q.; Morokuma, K.; Malick, D. K.; Rabuck, A. D.; Raghavachari, K.; Foresman, J. B.; Cioslowski, J.; Ortiz, J. V.; Stefanov, B. B.; Liu, G.; Liashenko, A.; Piskorz, P.; Komaromi, I.; Gomperts, R.; Martin, R. L.; Fox, D. J.; Keith, T.; Al-Laham, M. A.; Peng, C. Y.; Nanayakkara, A.; Gonzalez, C.; Challacombe, M.; W. Gill, P. M.; Johnson, B.; Chen, W.; Wong, M. W.; Andres, J. L.; Gonzalez, C.; Head-Gordon, M.; Replogle, E. S.; Pople, J. A. *Gaussian 98*, revision A.6; Gaussian, Inc.: Pittsburgh, PA, 1998.

(30) González, C.; Schlegel, H. B. *J. Phys. Chem.* **1989**, *90*, 2154.

(31) Sambrano, J. R.; Gracia, L.; Berski, S.; Beltrán, A. *J. Phys. Chem. A* **2004**, *108*, 10850.

(32) Contreras, R.; Fuentealba, P.; Galván, M.; Pérez, P. *Chem. Phys. Lett.* **1999**, *304*, 405.

(33) Fuentealba, P.; Pérez, P.; Contreras, R. *J. Chem. Phys.* **2000**, *113*, 2544.

(34) Böhland, T.; Temps, F.; Wagner, H. Gg. *Ber. Bunsen-Ges. Phys. Chem*. **1985**, *89*, 1100.

(35) We thank a reviewer for pointing out this important remark.

(36) Domingo, L. R.; Aurell, M. J. *J. Org. Chem*. **2002**, *67*, 959.

(37) Griesbeck, A. G.; Manabu, A.; Bondock, S. *Acc. Chem. Res*. **2004**, *37*, 919.